






INVESTIGATION OF THE EFFECTS OF RIB APPLICATION ON COOLING IN A TURBINE BLADE

^{1,2,*} Muhammed Emin TOLU , ² Osman BABAYİĞİT , ³ Dilek Nur ÖZEN 

^{1,2} Necmettin Erbakan University, The Graduate School of Natural and Applied Science, Mechanical Engineering Department, Konya, TÜRKİYE

² Karamanoğlu Mehmetbey University, Engineering Faculty, Mechanical Engineering Department, Konya, TÜRKİYE




³ Necmettin Erbakan University, Engineering Faculty, Mechanical Engineering Department, Konya, TÜRKİYE
^{1,2} metolu@kmu.edu.tr, ² obabayigit@kmu.edu.tr, ³ dnozen@erbakan.edu.tr

Highlights

- A rib turbulator cooling design was developed, and the solid model was created
- The mesh structure required for flow and heat transfer analyses was generated
- CFD analyses were conducted for both the ribbed and non-ribbed turbine blades
- Nondimensional temperature parameter (T/T_0) for both turbine blades were compared



INVESTIGATION OF THE EFFECTS OF RIB APPLICATION ON COOLING IN A TURBINE BLADE

^{1,2,*}Muhammed Emin TOLU , ²Osman BABAYİĞİT , ³Dilek Nur ÖZEN 

^{1,2}Necmettin Erbakan University, The Graduate School of Natural and Applied Science, Mechanical Engineering Department, Konya, TÜRKİYE

²Karamanoğlu Mehmetbey University, Engineering Faculty, Mechanical Engineering Department, Konya, TÜRKİYE

³Necmettin Erbakan University, Engineering Faculty, Mechanical Engineering Department, Konya, TÜRKİYE
^{1,2}metolu@kmu.edu.tr, ²obabayigit@kmu.edu.tr, ³dnozen@erbakan.edu.tr

(Received: 24.10.2024; Accepted in Revised Form: 22.02.2025)

ABSTRACT: Turbine blades are system components exposed to extremely high temperatures. Effective cooling of turbine blades is essential to enhance efficiency and extend the operational lifespan of gas turbines. In this study, a new rib turbulator cooling design was tested for the NASA C3X turbine blade. The analyses were compared with those conducted on non-ribbed blades. According to the findings, an average surface temperature of 574.6 K and a maximum surface temperature of 661.8 K were achieved. These values indicate a cooling efficiency of 19.1% for the leading edge, which is exposed to the maximum temperature, and 29.75% for the average surface temperature. All data obtained from the study have been shared in the form of figures and graphs.

Keywords: CFD Analysis, Ribbed Turbulators, Turbine Blade Cooling

1. INTRODUCTION

Throughout history, mankind, requiring increasing amounts of energy and power at each stage, has perpetually aimed to exert greater control over nature to sufficiently meet these needs. Humanity who had to produce various solutions to achieve this has scrutinized the functioning of nature and, pioneered numerous innovations, in the light of the information they acquired.

Presently, among the myriad mechanisms devised by humanity to fulfill its needs, gas turbines stand as prominent contributors. Gas turbines find application not only in electricity generation facilities but also in transportation. While their usage in land transportation is encountered, they are notably more extensively employed in aviation and maritime transport. Turbojet, turboprop, turboshaft, and turbofan engines utilized in transportation are specialized variants of gas turbine engines.

Gas turbines, fundamentally, are systems operating according to Newton's third law of motion, the principle of action and reaction. In gas turbines operating based on the Brayton cycle, the air compressed in the compressors reaches high pressure and high temperature. Subsequently, the air transferred to the combustion chamber is ignited with fuel. The resulting high energy is transferred to the turbine blades, facilitating the conversion of heat energy into mechanical energy. Then, the exhaust air is expelled from the exhaust.

Turbines consist of stationary blades (stator) and moving blades (rotor). Stationary blades intercept the flow before it reaches the moving blades, directing the airflow most efficiently towards the moving blades. Moving blades, on the other hand, facilitate the conversion of the heat energy acquired by the air in the combustion chamber into mechanical energy.

In gas turbines, turbine blades are particularly exposed to extremely high temperatures. The turbine inlet temperature is crucial not only for the power output and efficiency of the turbine but also significantly impacts the lifespan of turbine components. To achieve higher power and efficiency, it is increasingly desirable for gas turbines to operate at higher temperatures. The primary means to accomplish this is by enabling turbine blades to withstand these elevated temperatures.

*Corresponding Author: Muhammed Emin Tolu, metolu@kmu.edu.tr

For turbine blades to operate under higher temperatures, it is essential to reduce the thermal stresses they experience. Therefore, cooling of turbine blades, particularly the efficient cooling of stationary turbine blades (stators) which first encounter the high-temperature fluid, is critical. Efficient cooling of turbine blades not only increases their lifespan but also enhances system efficiency by enabling operation at higher temperatures.

Efficiently cooled turbine blades will have an extended service life, reduced maintenance costs, and enhanced turbine efficiency, enabling higher power output.

There are also some disadvantages associated with cooling applications in turbine blades. The air used for cooling is extracted from the compressor, which can reduce the power output obtained at the turbine exit. The introduction of cold air obtained from the compressor into the high-temperature fluid decreases the enthalpy and pressure values of the fluid, which can slightly impact turbine efficiency in a negative manner. Cooling applications also present various manufacturing challenges and lead to increased costs. Designing a cooling application that takes into account all these advantages and disadvantages will ensure the most efficient results.

Experimental studies on this subject in the literature are limited due to very high costs and a complex process. Despite this, the fact that humanity need more power day by day increases the importance of studies on cooling turbine blades and prompting scientists to focus more and more on this issue.

One of the pioneering studies on cooling turbine blades was undertaken by Hylton et al. [1]. In this experimental study, Hylton et al. selected three C3X turbine blades to simulate the first stage of a gas turbine and examined the effects of the channels on the cooling of the blade. Subsequent studies have referenced this experimental study and compared their own numerical data with the experimental data obtained by Hylton and colleagues for validation purposes.

In numerical simulations, selecting an appropriate turbulence model is crucial for simulating the flow. In a study by Menter et al. [2] in 1994, the SST $k-\omega$ turbulence model was first proposed as a blend of the $k-\omega$ and $k-\varepsilon$ turbulence models, aiming to combine the strengths of both models while avoiding their respective disadvantages.

In a study conducted by Faccini et al., [3] the thermal behavior of a NASA-C3X gas turbine blade, cooled radially by fluid passing through 10 cooling channels, was simulated using three-dimensional conjugate heat transfer simulations with the STAR-CD™ code. The study modeled the hot external flow volume and obtained the metal temperature distribution of the blade. The obtained data were compared with the results of experimental study, and the comparison results were presented graphically.

Referencing the study by Hylton et al., Zheng et al., [4] investigated five different turbulence models (standard $k-\varepsilon$, realizable $k-\varepsilon$, SST $k-\omega$, transitional $k-k\ell-\omega$, and v^2f) to simulate the airflow and heat transfer of a turbine guide vane. Based on the results obtained, it was noted that the SST $k-\omega$ turbulence model performed very well in accurately predicting heat transfer.

In a study conducted in 2016, Mazaheri et al., [5] optimized the shape and position of cooling channels in a C3X turbine blade. Their objective was to minimize the maximum temperature gradient and maximum temperature along the three-dimensional span of the blade. They modeled the shape of the cooling channels using a new method based on Bezier curves and utilized forty design variables in their study.

In their study titled "Optimization of Turbine Blade Cooling for Enhanced Turbine Performance," Mousavi et al., [6] simulated a simplified 2D model of the C3X blade to improve turbine performance. They conducted simulations using four different turbulence models, and the resulting data were compared with experimental data obtained by Hylton et al. in 1983. This comparison served as a validation study for their simulations.

Yousefi et al., [7] conducted research using computer-aided simulations to investigate the effects of ribbed channels on a modified NASA C3X gas turbine blade. In their study referencing the baseline design with ten cooling channels used by Hylton et al., they proposed a new model aimed to improve cooling performance by incorporating ribs of specific dimensions into the cooling channels. They studied the temperature distribution, convective heat transfer coefficient of the blade surface, performance factor, and

friction coefficient. Researchers examined six different configurations of longitudinally placed ribs within the cooling channels. They compared the obtained results with experimental results of Hylton et al., and numerical results of another previous study of Faccini et al. They found that these ribs increased heat transfer within the cooling channels by 25% while only increasing the friction factor by 3%. Additionally, the performance factor improved by 24%, and the maximum temperature was reduced by 25 K°.

In another study conducted in 2021, Karimi et al., [8] aimed to optimize an internally cooled gas turbine blade by enhancing cooling performance and reducing sensitivity to operational uncertainties. Using the v^2f turbulence model to minimize simulation errors, the researchers employed polynomial chaos methods for quantifying uncertainties. Their primary objective was to minimize the maximum temperature and maximum temperature gradient of the blades to extend their service life.

Vo et al., [9] simulated the combined heat transfer in the first-stage cooling blade of a W501F engine in their study, where they examined the effects of thermal barrier coating thickness and the ratio of the coolant flow to the mainstream hot gas pressure and temperature in blade film cooling. They found that a 100 K decrease in the coolant temperature resulted in an average blade temperature decrease of 58 K. Additionally, they determined that the presence of a thermal barrier coating with a thickness of 0.8 mm led to a 35% reduction in the heat transfer coefficient on the blade surface.

Goktepedi and Atmaca [10] investigated the phenomena of flow separation and reattachment over a backward-facing step through numerical modeling. They conducted the analysis at a Reynolds number of $Re=5000$, referencing a prior experimental study and employing the RNG $k-\epsilon$ turbulence model. As a result, they identified the reattachment length as 5,92 which aligns with the experimental data.

In this study, a new design of C3X turbine blade which features rib turbulators applied along the entire inner wall, was examined and the impact of the pressure and temperature of the coolant on blade cooling was investigated in a blade. The contributions to the literature resulting from this study are listed below:

- Cooling channels are used for the cooling of turbine blades. In this study, unlike other studies reviewed in the literature, the entire internal surface of the NASA C3X turbine blade has been modeled as a cooling channel for the cooling of the turbine blade.
- The ribbed cooling design used for the cooling of turbine blades was applied to the entire internal surface of the turbine blade, which was modeled as a cooling channel in a manner that has not been studied before.
- The obtained results were presented in the form of diagrams, tables, and graphs.

2. DESCRIPTION OF SYSTEM

Since the airflow reaching the turbine blades has extremely high temperatures, designing turbine blades to withstand such high temperatures is crucial for both the efficiency of the system and the operational lifespan of the blades. Numerous studies are being conducted across various fields to enhance the ability of turbine blades to withstand high temperatures. Some of these studies focus on manufacturing turbine blades from materials that can endure higher temperatures or coating the turbine blades with materials that are resistant to high temperatures, while others concentrate on cooling the blades to enable their operation even at extremely high temperatures.

As a result of numerous studies on turbine blade cooling, alternative cooling methods have been developed that can be applied under different operating conditions. Alnaeli et al., [11] adverted that the cooling process in turbine blades can be implemented through various methods which can generally be categorized into two main types as internal cooling and external cooling. The internal cooling methods that can be applied to a turbine blade are shown in the Figure 1.

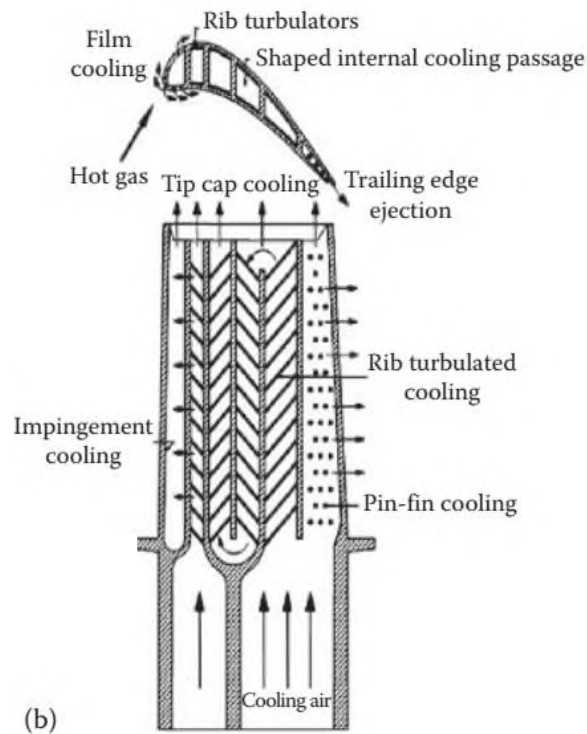


Figure 1. Various internal cooling methods used for cooling turbine blades [11]

The turbine blade to be used in this study was selected as the NASA C3X type, which has been used in numerous studies in the literature. Subsequently, a solid model of the turbine blade was created using the coordinate data obtained from the literature and with the aid of computer-aided solid modeling software, a ribbed turbulator design was applied to the internal surface of the blade, and flow domains for both the hot external flow and the cold internal flow were generated as can be observed in Figure 2.

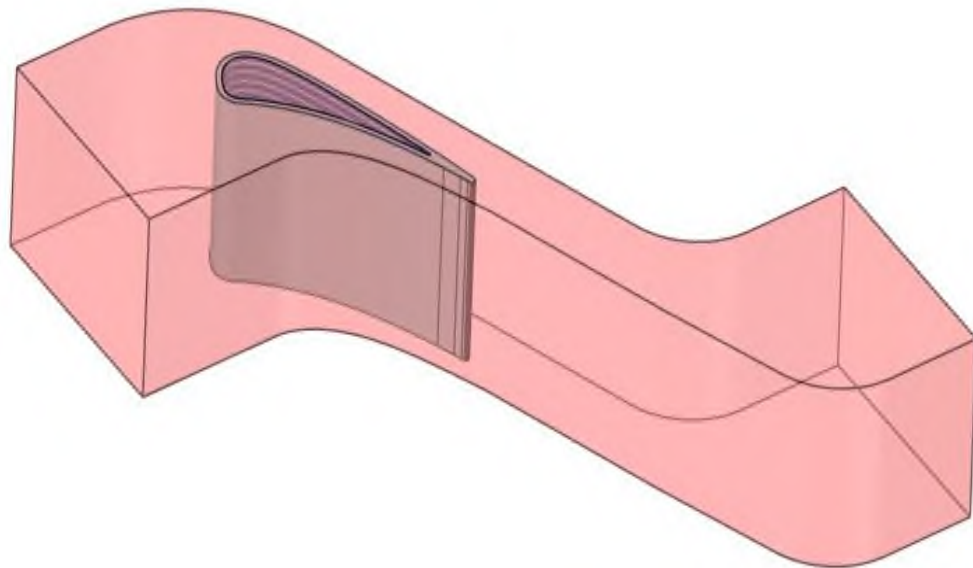


Figure 2. Turbine blade, hot external flow domain and cold internal flow domain

The flow analyses of the final design, which includes the solid model of the turbine blade with an

applied ribbed turbulator cooling design, as well as the internal and external flow volumes, were conducted using computer-aided simulations.

All the data obtained from the analyses, which examined heat transfer and pressure drops, were compiled in the form of graphs and diagrams.

3. MATERIAL AND METHOD

In this study, a NASA C3X type turbine blade was used, and a cooling design was investigated for this blade. The coordinates used for modeling the NASA C3X turbine blade were presented in the study conducted by Hylton et al. [1]. The geometric parameters of the NASA C3X turbine blade are provided in Table 1 [4].

Table 1. The geometrical parameters of NASA C3X turbine blade [4].

Blade Chord (mm)	Setting Angle (°)	Air Exit Angle (°)	Axial Chord (mm)	Vane Spacing (mm)	Throat (mm)
144.93	59.89	72.38	78.16	117.73	32.92

3.1. Design of the Cooling Method

As a result of the literature review, no study was found in which the entire internal surface of the turbine was designed as a cooling channel. In order to address this gap in the literature and introduce a novel cooling design, the entire internal surface of the turbine blade was conceptualized as a cooling channel, and rib turbulator design were applied along the inner surface of the blade. This approach aims to enhance cooling efficiency by maximizing heat transfer across the entire internal surface. The solid modeling of this design was created using the SolidWorks® design software and can be seen in Figure 3.

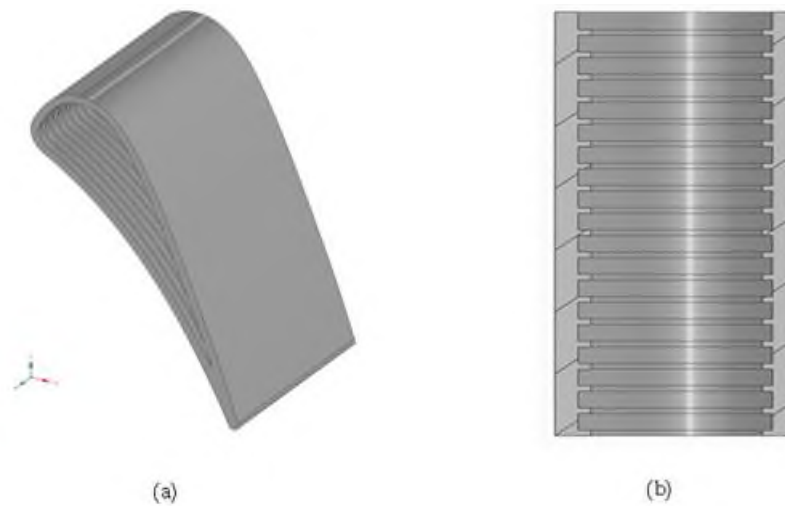


Figure 3. (a) turbine blade with rib turbulator, (b) cross-section of rib turbulator design.

There are several critical geometric parameters and design constraints that play a significant role in the design of ribbed turbulator cooling applications. These include the rib pitch-to-height ratio (p/e) and rib height-to-hydraulic diameter ratio (e/D). Each of these parameters must be optimized to balance between maximizing heat transfer and minimizing pressure drop.

As a result of the literature review [12], the geometric parameters were selected as follows: the "p" value, which represents the distance between two ribs, was chosen as 4 mm, and the "e" value, representing the rib height, was set to 1 mm. Accordingly, the rib pitch-to-height ratio (p/e) was determined to be 4.

The hydraulic diameter, which is required to calculate the e/D ratio, another design constraint

representing the ratio of rib height to hydraulic diameter, was determined using the following formula (1):

$$D = \frac{4A}{W} \quad (1)$$

Here; D , A and W are the hydraulic diameter, the cross-sectional area of the flow channel and the wetted perimeter of the channel respectively.

Both the A (cross-sectional area) and W (wetted perimeter) values were measured using the solid modeling program interface, with values of 1881.75 mm^2 and 260 mm , respectively.

The p/e ratio and the e/D ratio are crucial for the rib turbulator cooling channel design to ensure efficient cooling [12] and they are presented in Table 2.

Table 2. Design parameters of the rib turbulator application.

p/e	4
e/D	0.035

Additionally, the technical drawing and the geometric parameters of the rib turbulator cooling channel design can also be seen in Figure 4.

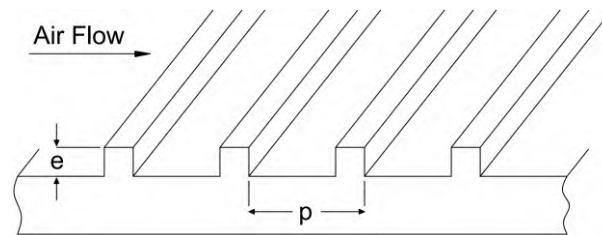


Figure 4. Geometric parameters of rib turbulator cooling channel

3.2. Design of the Analysis Domain

In order to perform the flow analysis, it is necessary to model the flow domain of the hot external flow coming onto the turbine blade. Based on the literature review, the design parameters used for the hot external flow domain in a study conducted by Zheng et al. using the NASA C3X turbine blade were referenced [4]. The domains of hot flow and cold flow are shown in Figure 5.

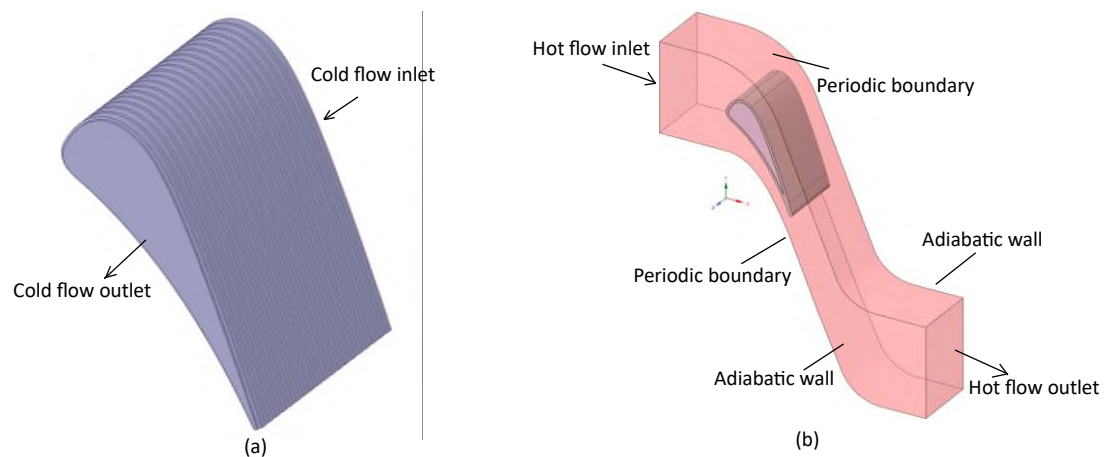


Figure 5.(a) Domain for internal flow, (b) external and internal flow domains with turbine blade

Cooling with rib turbulators is one of the most commonly used cooling techniques, which is an internal cooling method and employed in this study. In such cooling applications, an increase in cooling and heat transfer is expected by creating turbulence in the blade cooling canals [13]. The ribbed structure that creates turbulence is prepared as part of the manufacturing process and integrated into the blade during casting.

3.3. Computational Model

Modeled turbine blade and flow domains have been imported into the Ansys Fluent® program. Proper setup of the model within the program and accurate creation of the mesh structure are crucial for obtaining reliable analysis results.

The mesh structure was created using the Fluent Meshing module in the Ansys software. A poly-hexcore mesh was chosen to achieve a higher-quality flow analysis with a reduced number of elements. Based on the mesh independence study, an element count of 1371379 was selected as it provides the most efficient results with the lowest computational cost. The maximum skewness value of the generated mesh was 0.8285. A visual representation of the generated mesh structure is provided in Figure 6.

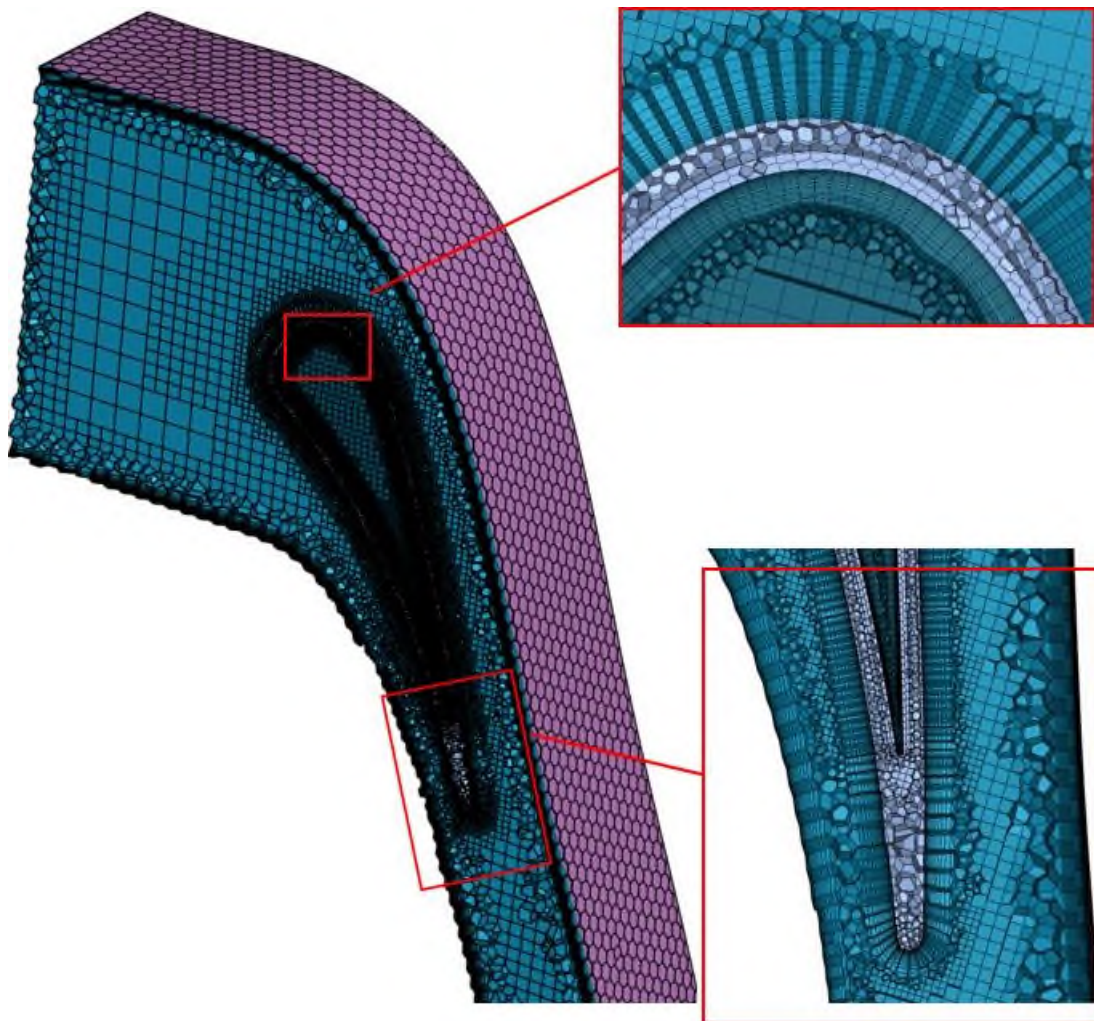


Figure 6. Mesh structure created for flow and heat transfer analyses

The flow analyses were conducted using the realizable $k-\epsilon$ turbulence model with the Menter-Lechner near-wall treatment method, achieving a y^+ value close to 30. The realizable $k-\epsilon$ model is a more realistic model which better represents the distribution of turbulent kinetic energy and energy dissipation [14]. In

addition, the realizable k - ϵ model provides greater accuracy near the wall and yields more consistent results in flow separation, reattachment, and recirculation regions [15].

At this stage of the study, the following assumptions and definitions have been made:

- Periodic boundaries have been defined, and adiabatic wall assumptions have been applied for the hot external flow domain.
- For the surfaces in contact with the flow, smooth surface and no-slip condition assumptions have been applied.
- The NASA C3X turbine blade is made of ASTM-310 stainless steel (OCr25Ni20), with a constant density of 8030 kg/m³ and a specific heat capacity of 502 J/kg·K [16]. The thermal conductivity value of blade (k_b) varies with temperature and is calculated using the linear equation (2) provided below

$$k_b = 0,0115T + 9,9105 \quad (2)$$

- Air is used as the cooling fluid and is assumed to behave as an ideal gas. Since the thermal conductivity (k_A), specific heat ($C_{p,A}$), and viscosity (μ_A) of air vary with temperature, these values were not entered as constants but were instead calculated using equations.

The thermal conductivity of air was calculated using the Sutherland's Formula (3) [17].

$$k_A = k_0 \cdot \left(\frac{T}{T_0} \right)^{3/2} \cdot \left(\frac{T_0 + S}{T + S} \right) \quad (3)$$

where k_A , k_0 , T , T_0 and S are; thermal conductivity at temperature, thermal conductivity at the reference temperature, temperature of the fluid, reference temperature and Sutherland constant respectively. A User Defined Function (UDF) code was written to implement the formula for calculating the thermal conductivity of air in the flow and heat transfer analyses. This code was embedded into the library of the analysis software.

The dynamic viscosity (μ_A) of air was calculated using the Sutherland's Formula (4) [17].

$$\mu_A = \mu_0 \cdot \left(\frac{T}{T_0} \right)^{3/2} \cdot \left(\frac{T_0 + S}{T + S} \right) \quad (4)$$

where μ_0 is Dynamic Viscosity at the reference temperature T_0 .

The specific heat capacity of air was calculated using the equation (5) provided below [4]:

$$C_{p,A} = a_0 + a_1 \cdot T + a_2 \cdot T^2 + a_3 \cdot T^3 + a_4 \cdot T^4 \quad (5)$$

The coefficients used in the calculation of specific heat are given in Table 3.

Table 3 . The coefficients used in the calculation of specific heat

a_0	a_1	a_2	a_3	a_4
957.110256	0.2365234	$5.141114 \cdot 10^{-6}$	$-3.3917446 \cdot 10^{-9}$	$-6.0929646 \cdot 10^{-12}$

- The boundary conditions for the hot external flow and cold internal flow, obtained from the literature review, are provided in the Table 4 below. P_{Hin} , T_{Hin} , Tu , Tv , P_{Hout} are inlet pressure, inlet temperature, turbulence intensity, viscosity ratio and outlet pressure of hot flow respectively. For the cold flow, V_{Cin} , T_{Cin} , Tu , D_H and P_{Cout} represent the inlet velocity, inlet temperature, turbulence intensity, hydraulic diameter, and outlet pressure, respectively.

Table 4. The boundary conditions of hot external flow and cold internal flow

	P_{Hin} (Pa)	T_{Hin} (K)	Tu (%)	Tv	P_{Hout} (Pa)
Hot external flow	413286	818	8.3	30	101325
	V_{Cin} (m/s)	T_{Cin} (K)	Tu (%)	D_{H} (mm)	P_{Cout} (Pa)
Cold internal flow	65.77	349.2	10	25.7	101325

3.4. Mathematical Model

The governing equations of motion for a continuous, viscous fluid are three-dimensional, time-dependent, compressible Navier-Stokes equations [18], [19], [20]. These equations are the continuity equation (6) [12];

$$\nabla \cdot (\rho \cdot \vec{V}) = 0 \quad (6)$$

the momentum equation (7) [12];

$$\nabla \cdot \left[(\rho \cdot v_i \cdot \vec{V}) - (\mu_{\text{eff}} \cdot \nabla v_i) \right] = \frac{\partial p}{\partial x_i} + S_{v_i} \quad (7)$$

and the energy equation (8) [12];

$$\nabla \cdot \left[(\rho \cdot T \cdot V) - (\alpha_{\text{eff}} \cdot \nabla T) \right] = S_T \quad (8)$$

where S_{v_i} and S_T are source term for the momentum transport equation in the i direction and source term for energy transport respectively.

The realizable k- ϵ turbulence model, chosen for flow analyses, includes transport equations for the turbulence kinetic energy (k) and the rate of turbulence dissipation (ϵ). The turbulence kinetic energy equation (9) is;

$$\frac{\partial(\rho \cdot k)}{\partial t} + \nabla \cdot (\rho \cdot k \cdot \vec{V}) = \nabla \cdot \left[\left(\frac{\mu + \mu_t}{\sigma_k} \right) \cdot \nabla k \right] + P_k - (\rho \cdot \epsilon) \quad (9)$$

where P_k is production term of turbulence kinetic energy.

ϵ is rate of turbulence dissipation and found with equation (10).

$$\frac{\partial(\rho \cdot \epsilon)}{\partial t} + \nabla \cdot (\rho \cdot \epsilon \cdot \vec{V}) = \nabla \cdot \left[\left(\frac{\mu + \mu_t}{\sigma_\epsilon} \right) \cdot \nabla \epsilon \right] + \left[(\rho \cdot C_1 \cdot S_\epsilon) - \left(\rho \cdot C_2 \cdot \frac{\epsilon^2}{k + \sqrt{v \cdot \epsilon}} \right) \right] \quad (10)$$

4. RESULTS AND DISCUSSION

The solid modeling of the NASA C3X ribbed turbulator turbine blade was performed using the SolidWorks CAD software, while the flow and heat transfer analyses were conducted in Ansys Fluent.

Figure 7 shows the pressure distribution of the refrigerant in the ribbed turbulator cooling channel. The rib turbulators within the cooling channel enhance cooling performance by increasing turbulence in the coolant, thereby improving heat transfer. However, the rib turbulators also cause a pressure drop in the coolant. The pressure drop in the coolant flow within the cross-sectional view of the cooling channel is can be seen in Figure 7.

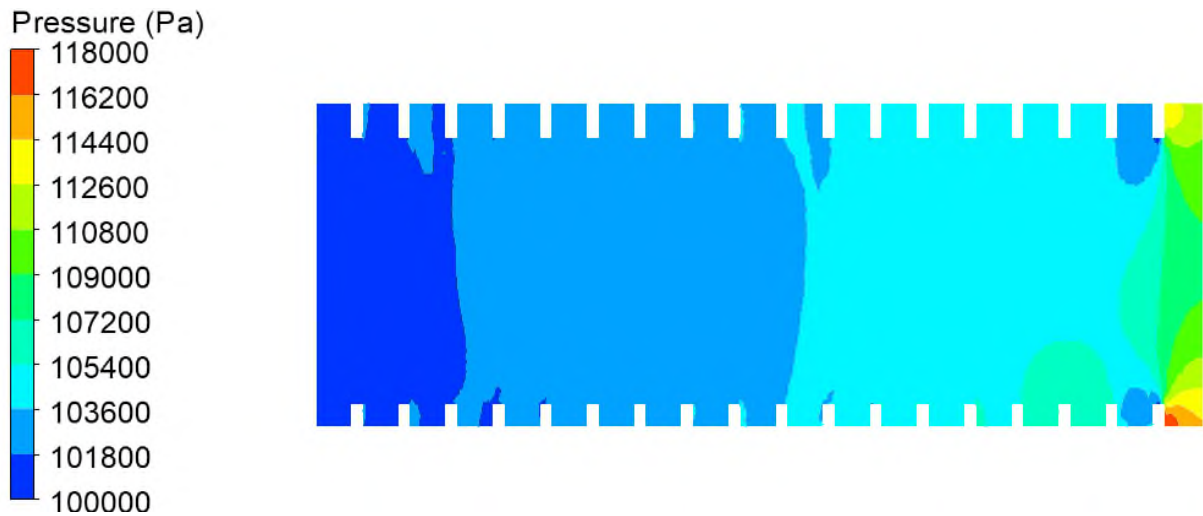


Figure 7. Pressure distribution of the coolant flow within the ribbed turbulator cooling channel

The inlet pressure and outlet pressure were measured and a pressure drop of 8100 Pa was recorded within the ribbed cooling channel, indicating a 7.4% pressure loss.

The pressure contour for the hot external flow is presented in Figure 8. The contour indicates that the leading edge of the blade is subjected to the highest pressure. In addition, as expected, the pressure values on the pressure side of the turbine blade remain significantly higher than those on the suction side. It can be observed that around the trailing edge, where the flow velocity is expected to reach its highest value, the pressure values decrease accordingly.

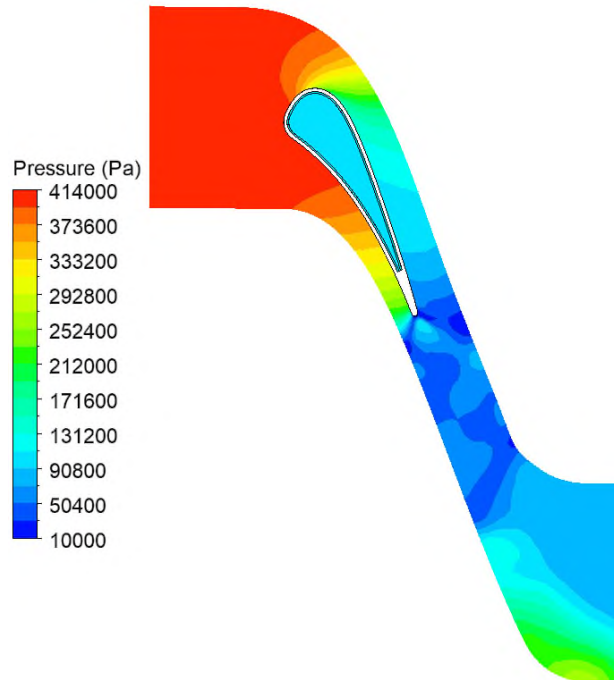


Figure 8. Pressure contour of the hot external flow obtained from flow analysis

The velocity contour obtained from the flow analyses is presented in Figure 9. It can be observed that at the leading edge, where pressure values are highest, velocity values are at their lowest. Conversely, at the trailing edge, as expected, the flow velocity reaches its maximum values. Additionally, in accordance with the no-slip condition, the velocity at the surfaces is observed to be zero. For the coolant, velocity values are also very low in the ribbed region.

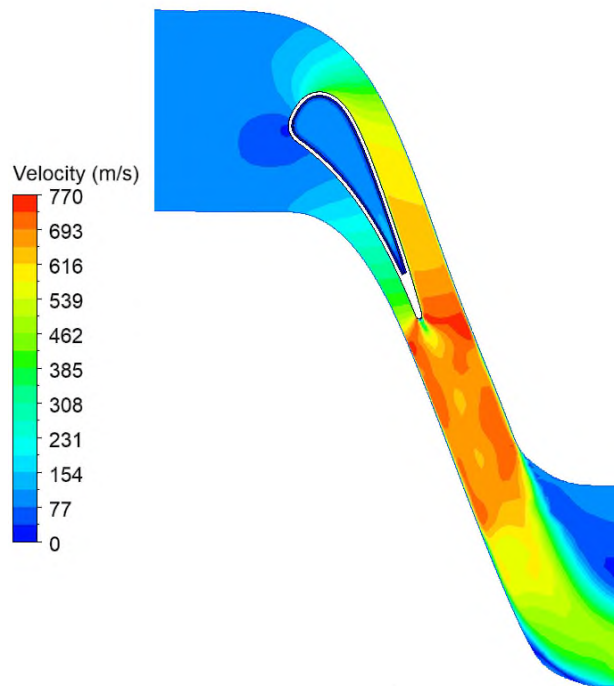


Figure 9. Velocity contour of the hot external flow and cold internal flow

The temperature contour obtained from the heat transfer analysis is shown in Figure 10. High temperature values are observed along the pressure side of the blade, where the flow adheres to the blade surface, while significant temperature drops are seen on the suction side, where flow separation occurs.

Examining the temperature contour of the turbine blade reveals that the coolant is highly effective in cooling the turbine blade. The area with the weakest cooling effect is the trailing edge, where rib turbulators could not be applied due to design constraints.

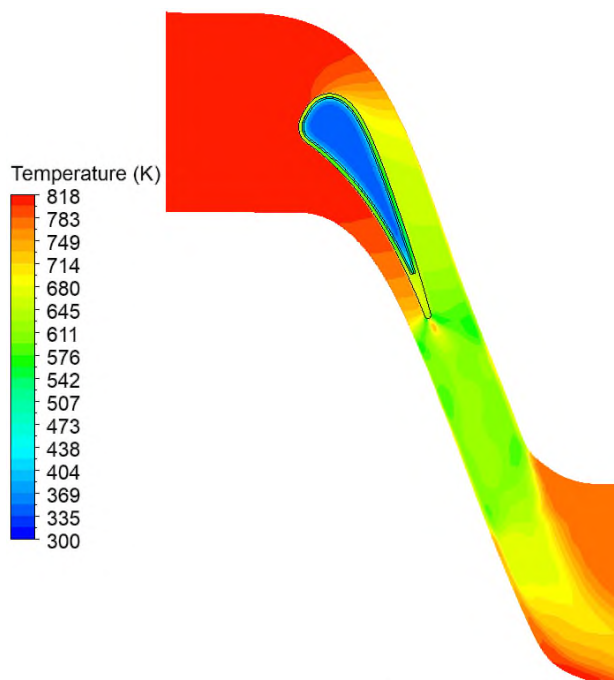


Figure 10. Temperature contour of the hot external flow and cold internal flow

The average surface temperature (T_{ave}) of the ribbed turbine blade was measured as 574.6 K, while

the maximum surface temperature (T_{max}) was determined to be 661.8 K. Given that the temperature of the hot external flow (T_{Hin}) is known to be 818 K, a temperature difference of 156.2 K is observed between the hot flow and the maximum surface temperature. This indicates a cooling performance of 19.1% even at the maximum surface temperature. For the average surface temperature of the blade, the cooling performance is 29.75%.

The comparison between the normalized temperature value graph of the turbine blade with a ribbed turbulator cooling channel and the normalized temperature value graph of the turbine blade cooled with a non-ribbed cooling channel is presented in Figure 11.

The normalized temperature value graphs were obtained by calculating the ratio of the temperature at any point on the blade surface (T) to the reference temperature ($T_0=818$ K) for both blades.

The graph shows that the greatest difference in cooling efficiency between the turbine blade with a ribbed turbulator cooling channel and the one without is observed at the leading edge and nearby regions. As the trailing edge, where ribs could not be applied, is approached, the cooling values for both turbine blades become nearly identical.

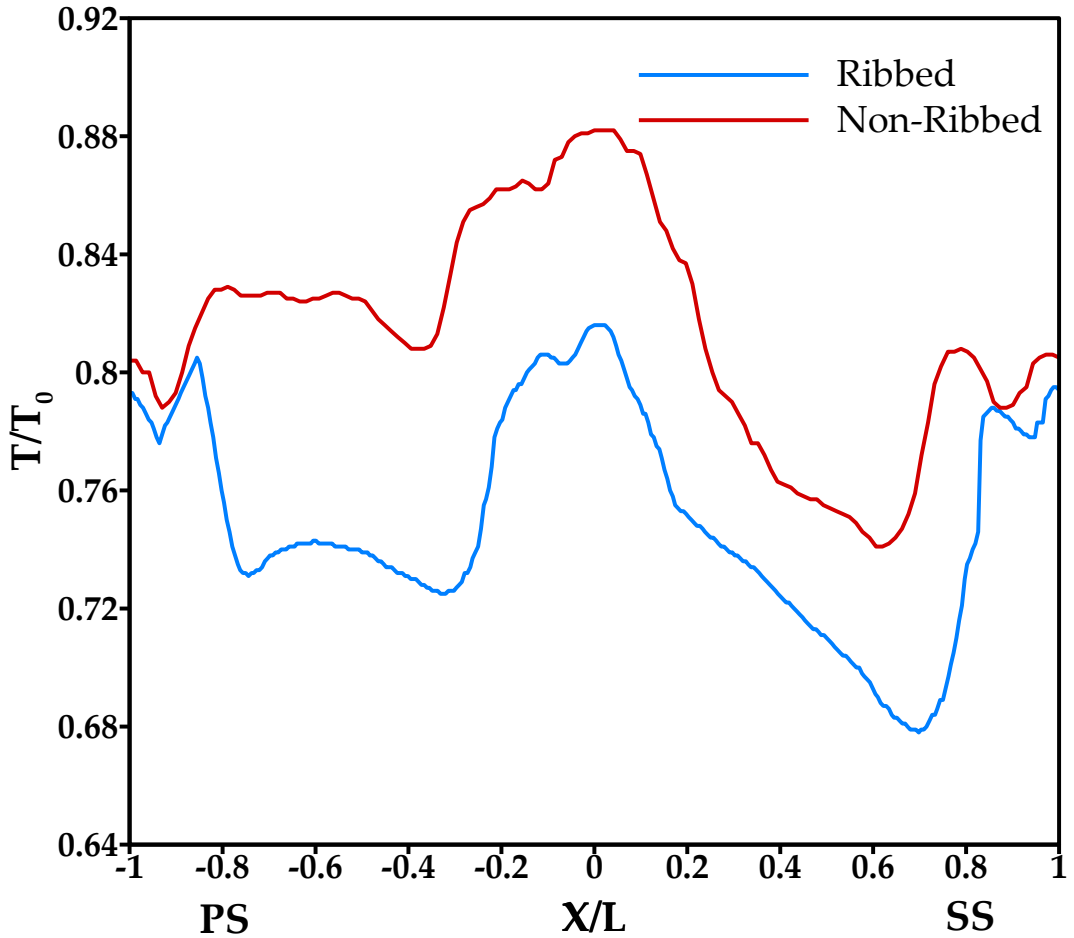


Figure 11. Comparison of normalized temperature values along the pressure and suction sides for ribbed and non-ribbed channels

5. CONCLUSION

In this study, flow and heat transfer analyses were conducted on a NASA C3X turbine blade made of ASTM-310 stainless steel. In these analyses, where the entire internal region of the turbine blade was designed as a cooling channel, pressure drop and heat transfer were examined for turbine blades with ribbed and non-ribbed cooling channels. The obtained data have been provided within the text and

presented in the form of figures and graphs.

1. The results indicate that the rib turbulators cause a 7.4% pressure drop in the cooling channel, while providing a 29.75% improvement in average surface cooling.
2. Due to design constraints, the trailing edge, where rib turbulators could not be applied, was observed to be the least cooled region of the blade. It is anticipated that if this region could be effectively cooled, the overall cooling efficiency would be significantly enhanced.
3. While the pressure drop caused by the rib turbulators is not overly significant compared to the cooling efficiency they provide, it is possible to reduce this pressure drop by making various design adjustments and optimization efforts in the rib design.

In our next study, further research on innovative blade and cooling channel designs to improve cooling efficiency in turbine blades is planned.

Declaration of Ethical Standarts

Authors declare that all ethical standards have been complied with.

Credit Authorship Contribution Statement

Muhammed Emin Tolu: Investigation, Modeling, Analyses, Writing.

Osman Babayiğit: Investigation, Supervision, Review, Editing.

Dilek Nur Özen: Investigation, Supervision, Review, Editing.

Declaration of Competing Interest

The authors declare that there are no declarations of interest.

Funding / Acknowledgements

The authors have not disclosed any funding. The authors acknowledged that this study is derived from the PhD Thesis of Muhammed Emin Tolu.

Data Availability

The data obtained from this study are available from the corresponding author upon reasonable request.

REFERENCES

- [1] L. D. Hylton, M. S. Mihelc, E. R. Turner, D. A. Nealy, and R. E. York, "Analytical and experimental evaluation of the heat transfer distribution over the surfaces of turbine vanes," NASA Lewis Research Centre, NASA-CR-168015, 1983.
- [2] F. R. Menter, "Two-equation eddy viscosity turbulence models for engineering applications," *AIAA Journal*, vol. 32, no. 8, pp. 1598–1605, 1994.
- [3] B. Facchini, A. Magi, and A. Scotti Del Greco, "Conjugate heat transfer simulation of a radially cooled gas turbine vane," in *ASME Turbo Expo 2004: Power for Land, Sea, and Air*, Vienna, Austria, Jun. 2004, pp. 951-961, vol. 3.
- [4] S. Zheng, Y. Song, G. Xie, and B. Sunden, "An assessment of turbulence models for predicting conjugate heat transfer for a turbine vane with internal cooling channels," *Heat Transfer Research*, vol. 46, no. 11, pp. 1039-1064, 2015.
- [5] K. Mazaheri, M. Zeinalpour, and H. R. Bokaei, "Turbine blade cooling passages optimization using reduced conjugate heat transfer methodology," *Applied Thermal Engineering*, vol. 103, pp. 1228-1236, 2016.

- [6] S. M. Mousavi, A. Nejat, and F. Kowsary, "Optimization of turbine blade cooling with the aim of overall turbine performance enhancement," *Energy Equipment and Systems*, vol. 5, no. 1, pp. 71-83, 2017.
- [7] A. Yousefi, A. Nejat, and M. H. Sabour, "Ribbed channel heat transfer enhancement of an internally cooled turbine vane using cooling conjugate heat transfer simulation," *Thermal Science and Engineering Progress*, vol. 19, Art. no. 100641, 2020.
- [8] M. S. Karimi, M. Raisee, S. Salehi, P. Hendrick, and A. Nourbakhsh, "Robust optimization of the NASA C3X gas turbine vane under uncertain operational conditions," *International Journal of Heat and Mass Transfer*, vol. 164, Art. no. 120537, 2021.
- [9] D. T. Vo, D. T. Mai, B. Kim, and J. Ryu, "Numerical study on the influence of coolant temperature, pressure, and thermal barrier coating thickness on heat transfer in high-pressure blades," *International Journal of Heat and Mass Transfer*, vol. 189, Art. no. 122715, 2022.
- [10] İ. Göktepe and U. Atmaca, "Numerical modeling of backward-facing step flow via computational fluid dynamics," *Journal of Scientific Reports-A*, vol. 054, pp. 176-193, 2023.
- [11] M. Alnaeli et al., "High-temperature materials for complex components in ammonia/hydrogen gas turbines: a critical review," *Energies*, vol. 16, no. 19, Art. no. 6973, 2023.
- [12] J.-C. Han, S. Dutta, and S. Ekkad, *Gas Turbine Heat Transfer and Cooling Technology*.
- [13] K. Tekin, "Gaz türbinleri kanatlarındaki soğutma tekniklerinin araştırılması," Master's Thesis, Sakarya Üniversitesi, 2020.
- [14] D. C. Wilcox, *Turbulence Modeling for CFD*. DCW Industries, 1998.
- [15] T. H. Shih, W. W. Liou, A. Shabbir, Z. Yang, and J. Zhu, "A new $k-\epsilon$ eddy viscosity model for high Reynolds number turbulent flows," *Computers & Fluids*, vol. 24, no. 3, pp. 227-238, 1995, doi: 10.1016/0045-7930(94)00032-T.
- [16] A. Goldsmith, T. E. Waterman, and H. J. Hirshhorn, *Handbook of Thermophysical Properties of Solid Materials*, vol. II: Alloys, New York: The Macmillian Company, 1961.
- [17] M. Lappa, "A mathematical and numerical framework for the analysis of compressible thermal convection in gases at very high temperatures," *Journal of Computational Physics*, vol. 313, pp. 687-712, 2016, doi: 10.1016/j.jcp.2016.02.062.
- [18] H. Schlichting, *Boundary Layer Theor*, McGraw-Hill Book Company, Inc., 1960.
- [19] J. E. Bardina, P. G. Huang, and T. Coakley, "Turbulence modeling validation," in *28th Fluid Dynamics Conference*, Jun. 1997, p. 2121.
- [20] Y. M. Ahmed and A. H. Elbatran, "Numerical study of the flow field characteristics over a backward facing step using $k-k_l-\omega$ turbulence model: comparison with different models," *World Journal of Engineering*, vol. 15, no. 1, pp. 173-180, 2018.